Hindawi Publishing Corporation
Journal of Nanomaterials
Volume 2016, Article ID 6304096, 10 pages
http://dx.doi.org/10.1155/2016/6304096

Research Article

Comparison of Acid Red 114 Dye Adsorption by Fe_3O_4 and Fe_3O_4 Impregnated Rice Husk Ash

Gul Kaykioglu and Elcin Gunes

Department of Environmental Engineering, Faculty of Corlu Engineering, Namik Kemal University, Corlu, 59860 Tekirdag, Turkey

Correspondence should be addressed to Gul Kaykioglu; gkaykioglu@nku.edu.tr

Received 29 April 2016; Revised 17 June 2016; Accepted 21 July 2016

Academic Editor: Xingmao Ma

The removal of Acid Red 114 (AR114) dye by adsorption process, using the magnetic nanoparticle (RHA-MNP) which is produced from rice husk ash burned at 300°C and the magnetic nanoparticle (MNP, Fe_3O_4), was studied. Batch processes were used under different test parameters: pH (2, 4, 6, and 10) and without pH, initial dye concentration (20, 40, 60, 80, and 100 mg/L), and contact time (0, 1, 5, 10, 15, 30, 45, 60, 90, and 150 min). Optimum conditions for AR114 removal were found to be at natural pH (pH without correction) for both adsorbents. Freundlich isotherm was found to be more consistent for MNP and Langmuir isotherm was found to be more consistent for RHA-MNP. The maximum adsorption capacities of MNP and RHA-MNP adsorbents for AR114 dye were equal to 111 mg/g. The kinetic experimental data fitted the pseudo-second-order model for both MNP and RHA-MNP. It can be concluded that RHA-MNP which is a waste could be used as low-cost adsorbent to remove AR114 from aqueous solution.

1. Introduction

Dyes are widely used in textile, plastic, food, cosmetics, paper, and carpet industries. The existence of dyes in the wastewater creates significant environmental problems. Dyes resist biodegradation with biological treatment. Coagulation-flocculation which includes chemical and physical methods, advanced oxidation processes like Fenton process (H_2O_2 + Fe^{+2}), membrane processes, and electrochemical methods are effective in the removal of dyes. However, these processes have some disadvantages such as being expensive and producing excessive amount of sludge. Most of the existing processes are adsorption processes, and generally activated carbon (AC) is used as the adsorbent in these processes [1]. Some researchers have investigated the usage of the agricultural wastes as the raw materials to produce activated carbon, which has a high adsorption capacity. In Turkey, the annual average production amount of rice is 700,000 tons. Disposal of rice husks is done in landfill sites, which causes an aesthetic pollution, eutrophication, and problems in aquatic life. Rice husks do not dissolve in water. They show silica-cellulose, ligneous, and corrosive characteristics. The most important materials that compose the internal structure of the rice husk are cellulose, hemicellulose, lignin, hydrated silica, and the ash content [2]. The adsorbent, which is obtained from rice husk, can be a good alternative for the activated carbon applications [1–8].

Magnetic nanoparticles can also be used in adsorption process as adsorbent. The features of the nanoparticles, whose sizes are less than 100 nm, are far more favorable than the features of the materials that have higher volumes. By the recent improvements in nanotechnology, the types of nanoparticles are synthesized successfully and gained attention to solve some of the environmental problems (acceleration of the coagulation of sludge, adsorption of radio nucleotides and organic dyes, and remediation of contaminated soil). Magnetic nanoparticles have large surface areas, highly magnetic characteristics, and high removal efficiencies. In addition, they have an advantage as the speedy and easy removal of the adsorbent from the solution (by the help of magnetic field). Also, compounds can be removed from the magnetic particles and can be reused [9–11]. There are some studies (AC/TiO_2, GAC/ZrO_2, TiO_2/sepiolite, and chitosan/ZnO) which prove that nanotechnological applications improved

the adsorbent feature of the adsorbents, which are prepared in order to be used in adsorption practices [12–15]. Generally, it is difficult to use the adsorbents in the systems, which are constantly in flow, due to their small particle diameters. Various studies have used the adsorbents in adsorption applications by combining them with iron oxide. Wang et al. (2011) [16] developed an adsorbent (bamboo ash used as a support material for iron) by using microwave. The low-cost, composite material that is obtained from $Fe_2(SO_4)_3$ and H_2SO_4 was used for the removal of Cr. BET specific surface area, total pore volume, and the average diameter of mesoporous of adsorbent are recorded and it was observed that all of them were decreased after the formation with iron. Absalan et al. (2011) [17] studied the removal of Ni(II) from the aqueous solutions by the adsorbents that are produced from the tea wastes, which are agricultural biomasses, and transformed into nanoparticles. Magnetic nanoparticles (Fe_3O_4) are produced from the chemical precipitation of Fe^{+2} and Fe^{+3} in an ammoniac solution. It was observed that when the concentration of Ni solution increased from 50 mg/L to 100 mg/L, the efficiency of the removal decreased from 99% to 87%. As a result of the study, the magnetic particles produced from tea wastes are efficient to remove the metals. Gupta and Nayak (2012) [18] produced a magnetic nanoparticle (MNP-OPP) by applying Fe_3O_4 nanoparticles together with the orange peel powder (OPP), which is an agricultural waste. The physicochemical features for metal binding capacity of the obtained magnetic adsorbent were observed. MNP-OPP is found to be more efficient to use rather than the application of MNP and OPP separately. Study has shown that the removal of cadmium (from simulated electronic industry wastewater) is 82%. As a result of the study, the feasibility of MNP-OPP has shown that it can easily be synthesized. Also, it is economic, environment friendly, and recyclable, and it can be used as an advanced adsorbent in order to prevent environment related problems. Do et al. (2011) [19] studied the adsorption performance of active carbon/composite Fe_3O_4 nanoparticles observed for methyl orange. It was stated that composites have large specific surface area, porosity, and good magnetic features.

In industrial districts of Turkey, aquatic life has been damaged and visual pollution has increased because of discharging colored effluents to surface waters. So color parameter has been added to Water Pollution Control Regulations and the necessity of putting an emphasis to the studies related to the removal of color has become evident. In Turkey, there is a need for doing a research related to the removal of the dyes from wastewater of textile industries especially after the addition of color parameter into discharge limits. According to the literature research, adsorption studies that have been done with magnetic nanoparticles are mostly on the removal of metals. Also, a study related to the removal of the color with magnetic nanoparticles that is obtained by the usage of rice husk ash as a support material is not found. In this study, the adsorption process in order to achieve the removal of the color of the aqueous solution prepared with the Acid Red 114 dye, widely used in textile industry, by the usage of magnetic nanoparticle (MNP, Fe_3O_4) and magnetic nanoparticle impregnated rice husk ash burned at 300°C (RHA-MNP) was studied.

Table 1: Physical and chemical features of AR 144.

Commercial name	Acid Red 114
Molecular formula	$C_{37}H_{28}N_4O_{10}S_3Na_2$
Purity	80%
Chromophore	Diazo
Molecular weight	830
λ_{max} (nm)	522
View	Dark red powder

2. Materials and Methods

2.1. Preparation of Adsorbents. The rice husk used in this study was obtained from a rice processing factory in the district of Uzunköprü, Edirne, Turkey. Raw rice husks were washed with a stream of distilled water to remove dirt, dust, and superficial impurities and then dried in an oven at 105°C for 24 h. Rice husks were carbonized in air in a muffle furnace (NÜVE MF120) at 300°C for 45 min (RHA) and cooled to room temperature.

6.1 grams of $FeCl_3 \cdot 6H_2O$ and 4.2 grams of $FeSO_4 \cdot 7H_2O$ were dissolved in 100 mL of water and heated up to 90°C. 10 mL 26% of ammonium hydroxide and the solution of 1 gram of rice husk ash (RHA) in 200 mL of water were added to each other quickly. pH was fixed to 10. The mixture was mixed for 30 minutes at 80°C and cooled down to room temperature. The obtained magnetic nanoparticle (RHA-MNP) was left for the settlement for 1-2 minutes and then washed with 100 mL of distilled water for 3 times. After that, the solution, the supernatant of which is filtered and separated, is dried at 50°C [18]. MNP was prepared by the same procedure, but RHA was not added.

2.2. Adsorbate and Batch Adsorption Studies. The adsorbate AR114 was obtained from Sigma-Aldrich. Physical and chemical features of Acid Red 114 are given in Table 1. The chemical structure of the dye AR114 is shown in Figure 1 [20]. 200 mg/L of stock solution was prepared to be used in adsorption applications. Solutions of the required concentrations (20–100 mg/L) were prepared by successive dilution of this stock solution.

Adsorption studies were carried out at various initial concentrations (20, 40, 60, 80, and 100 mg/L) and different pH conditions (without pH correction and pH values 2, 4, 6, and 10). Sampling intervals were set as 0, 1, 5, 10, 15, 30, 45, 60, 90, and 150 minutes. pH adjustment was done with 0.1 N HCl and 0.1 N NaOH. After adsorption studies MNP and RHA-MNP were removed from the solution using a magnet. Although high removal efficiency of magnet is performed, centrifuge (CN180 Nüvefuge) is also applied at 3,500 rpm for 5 min. The color measurement was done using a calibration curve prepared at the corresponding maximum wavelength of 522 nm in spectrophotometer (Thermospectronic Aqua-Mate Spectrometer).

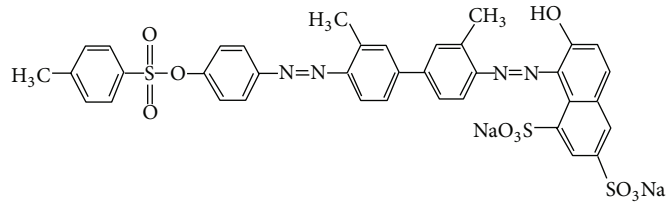

Figure 1: Chemical formula of Acid Red 114 dye.

2.3. Analysis. The examination of the adsorbents by scanning electron microscope (SEM) was done with the model device FEI Quanta FEG 250. The samples were examined without a preliminary preparation with the low vacuum detector (LFD) in low vacuum mode (20–80 Pascals), without coating with metals in different augmentations.

For the element analysis of the adsorbents, a device called Optical Emission Spectrometer (ICP-OES) from the brand named as Spectro was used. A microwave assisted digestion procedure was carried out with HNO_3/HCl mixture according to EPA 3051 A. 0.5 g sample was weighed out in the reaction vessel. 9 mL of HNO_3 and 3 mL HCl were then added to each vessel. Vessels were placed in the rotor and placed in the microwave. The vessels were heated to at least 175°C over 5.5 minutes and then held at 180°C for at least 4.5 minutes. After cooling, the resulting solutions were diluted up to 25 mL in volumetric flasks with ultrapure water.

Descriptive information about the bonds of the molecular or the compounded structures of the adsorbents was obtained from technique called ATR (attenuated total reflectance) in the device (BRUKER VERTEX 70 FT-IR ATR) of Fourier transform infrared spectroscopy (FT-IR).

After adsorption process, the dye concentration was measured at a wavelength corresponding to the maximum absorbance of AR114 (λ_{max} of 522 nm) using a Thermospectronic AquaMate Spectrometer.

2.4. Adsorption Equilibrium Studies. Adsorption equilibrium studies were carried out at initial concentrations of 20, 40, 60, 80, and 100 mg/L, without pH correction, at 90 minutes for MNP and 120 minutes for RHA-MNP and at fixed adsorbent doses of 0.2 g/200 mL (1 g/L). Adsorption equilibrium studies were employed to determine the adsorption capacity of the adsorbents by using Langmuir and Freundlich isotherm models. Langmuir isotherm, assuming that the adsorbent surface is resembled by means of the energy, was used to explain single-layered homogenous adsorption. It also helps to estimate the maximum adsorption capacity, and it is expressed as follows [24]:

$$q_e = \frac{(q_{\max} K_L C_e)}{(1 + K_L C_e)}. \quad (1)$$

q_e (mg/g) expresses the AR114 amount that each unit adsorbent adsorbs in the equilibrium condition, C_e (mg/L) stands for the AR114 concentration that remains in the solution after the adsorption when the equilibrium condition is reached, K_L (L/mg) is the equilibrium constant, and $q_{\max}$ expresses the adsorbate amount (mg/g) that is needed for single-layered form [25].

Langmuir equation is linearized as follows:

$$\frac{1}{q_e} = \frac{1}{q_{\max} K_L C_e} + \frac{1}{q_{\max}}. \quad (2)$$

Experimental results, $q_{\max}$ versus K_L values, were calculated by plotting of $1/q_e$ against $1/C_e$ [1].

Freundlich model is an empirical equation that is used to estimate the concentration of the adsorbent which can be observed on the surface of the adsorbent. Freundlich model and the linearized Freundlich equation are given below [26]:

$$q_e = K_f C_e^{1/n}, \qquad \log q_e = \frac{1}{n} \log C_e + \log K_f. \quad (3)$$

C_e is color concentration in the solution after the adsorption process (mg/L), q_e is adsorbed amount of material that is on the unit adsorbent (mg/g), K_f is adsorption capacity that is calculated in the experiments, and n is adsorption density.

Plot of $\ln C_e$ against $\ln q_e$ yields a straight line which indicates the adaptation of the Freundlich model. The value of n indicates the affinity of the adsorbate toward the adsorbent. $1/n$ and K_f can be calculated from the slope and intercept, respectively [1].

2.5. Adsorption Kinetics. In the study pseudo-first-order and pseudo-second-order models were used to analyze the adsorption kinetics of AR114. Lagergren equation is probably the first known method to estimate the adsorption speed in liquid phased systems. It is a commonly used equation for the first-order kinetics and expressed as follows [27]:

$$\frac{d_{q_t}}{dt} = k_1 (q_e - q_t). \quad (4)$$

k_1 is pseudo-first-order adsorption rate constant ($\min^{-1}$), q_e is the amount that is adsorbed in equilibrium condition (mg/g), and q_t is the adsorbed amount at time t (mg/g). The equation is integrated into form (4), using the boundary conditions $t = 0$, $q_t = 0$ and $t = t$, $q_t = q_t$:

$$\log (q_e - q_t) = \log q_e - \frac{k_1}{2.303} t. \quad (5)$$

The line that is drawn in the graph of t against $\log(q_e - q_t)$ helps calculating $q_{e,\text{calc}}$ and k_1 from the slope of the graph.

Table 2: Chemical characterization of MNP and RHA-MNP.

Sample	%									
	Si	S	P	Al	Ti	Fe	Ca	Mg	Na	K
MNP	0.002	0.5	0.0005	0.01	0.000015	62.99	0	0.0027	0.000005	0.0075
RHA-MNP	0.09	1.58	0.003	0.06	0.79	40.10	0.015	0.014	0.0026	0.127

The integrated form of the pseudo-second-order adsorption kinetic equation for the boundary conditions, from $t = 0$ to $t = t$ and from $q_t = 0$ to $q_t = t$, is as follows [1]:

$$\frac{d_{q_t}}{dt} = k_2 \left(q_e - q_t\right)^2, \tag{6}$$

$$\frac{1}{\left(q_e - q_t\right)} = \frac{1}{q_e} + kt, \tag{7}$$

$$\frac{1}{q_t} = \frac{1}{k_2 q_e^2} + \frac{1}{q_e} t. \tag{8}$$

If the initial adsorption rate is h (mg/g), (8) is expressed as (10):

$$h = k_2 q_e^2, \tag{9}$$

$$\frac{t}{q_t} = \frac{1}{h} + \frac{1}{q_e} t. \tag{10}$$

$q_{e,\mathrm{calc}}$ and k_2 can be estimated from the slope of the tangent line which is drawn to the slope of t against t/q_t graph.

3. Results and Discussions

3.1. Characteristics of Adsorbents. Chemical characterization of MNP and RHA-MNP is shown in Table 2. Carbonyl groups are the main function groups in ash. They decrease with the increasing burning temperature. This phenomenon contributes to the decrease in surface hydroxyl groups [28]. The surface area of rice husk ash depends on the amorphous carbon that is formed during the burning process.

SEM images give information about the morphology of the adsorbent. On the other hand they are also expected to be compatible with adsorption isotherm. SEM images shown in Figure 2 were taken at 100x and 5,000x magnification to observe the surface morphologies of raw rice husk, rice husk ash burned at 300°C, MNP, RHA-MNP, and MNP and RHA-MNP after adsorption process (MNP-A and RHA-MNP-A). According to the morphological assessment based upon the SEM images, the image of the raw rice husk without any heat treatment resembles an image of a corncob and the rice husk has protruding pattern like regular round shaped hills. The burning process of the rice husk was not completely done and the skeleton of the rice husk was not destroyed completely yet at 300°C. As a result of the burning process the patterns became more distinct. Magnetic nanoparticles contain nanosized pores (Figure 2(c)). After the adsorption process, pores on the surface of the magnetic nanoparticles decreased and planar formations occurred.

Although RHA-MNP structurally resembles MNP, it can be stated that rice husk ash settles on the active pores of MNP. Besides, due to the dyes that were engaged to the pores, RHA-MNP-A contained fewer pores and showed more homogenous structure (Figure 2(f)). The surface of MNP-A is heterogeneous structure (Figure 2(d)).

Table 3: pH variations after adsorption onto MNP and RHA-MNP (without pH correction).

Initial dye concentration (mg/L)	pH after adsorption with MNP (t = 90 min)	pH after adsorption with RHA-MNP (t = 150 min)
20	4.37	3.41
40	4.38	3.42
60	4.47	3.48
80	4.48	3.49
100	4.49	3.52

FT-IR spectrum shows the functional groups that exist in the structure of adsorbent. FT-IR spectrum results for RHA and MNP-RHA are shown in Figures 3 and 4. A peak was observed for 3128 cm^{-1} for MNP, which shows the aliphatic groups in MNP [29]. The same peak was observed for 3011 cm^{-1} for RHA-MNP. Peaks smaller than 700 cm^{-1} are related to the bonds of Fe-O in iron oxides and those peaks are observed for each adsorbent. Magnetic nanoparticles have two intense peaks. Those peaks are 632 cm^{-1} and 585 cm^{-1} [17]. This peak for MNP was observed as 552 cm^{-1} and for RHA-MNP it was observed as 551 cm^{-1}.

3.2. The Effect of pH, Initial Dye Concentration, and Contact Time on Adsorption. The point of zero charge ($\mathrm{pH}_{\mathrm{pzc}}$) is a significant parameter to explain adsorption of anions and cations under different pH values. The net total particle charge is zero at this point. This parameter helps to explain the mechanism of adsorption of anions and cations in the adsorption applications. In this study the $\mathrm{pH}_{\mathrm{pzc}}$ was estimated by the mass titration method [30]. The $\mathrm{pH}_{\mathrm{pzc}}$ values of the adsorbents MNP and RHA-MNP were found to be 4.5 and 3.5, respectively.

The pH of the solution is an important parameter in determining the adsorption properties of adsorbents. Table 3 shows natural pH according to initial AR114 concentration and adsorption processes onto MNP and RHA-MNP. As it can be seen from Table 3 after adsorption onto MNP pH reaches 4.5 which was $\mathrm{pH}_{\mathrm{pzc}}$ of MNP and after adsorption onto RHA-MNP pH reaches 3.5 which was $\mathrm{pH}_{\mathrm{pzc}}$ of RHA-MNP. As can be seen from Figure 5, the maximum q_e values were obtained without changing pH of the solutions. This can be explained by low solubility of MNP and RHA-MNP at $\mathrm{pH}_{\mathrm{pzc}}$ [31] and by the ligand exchange originating between

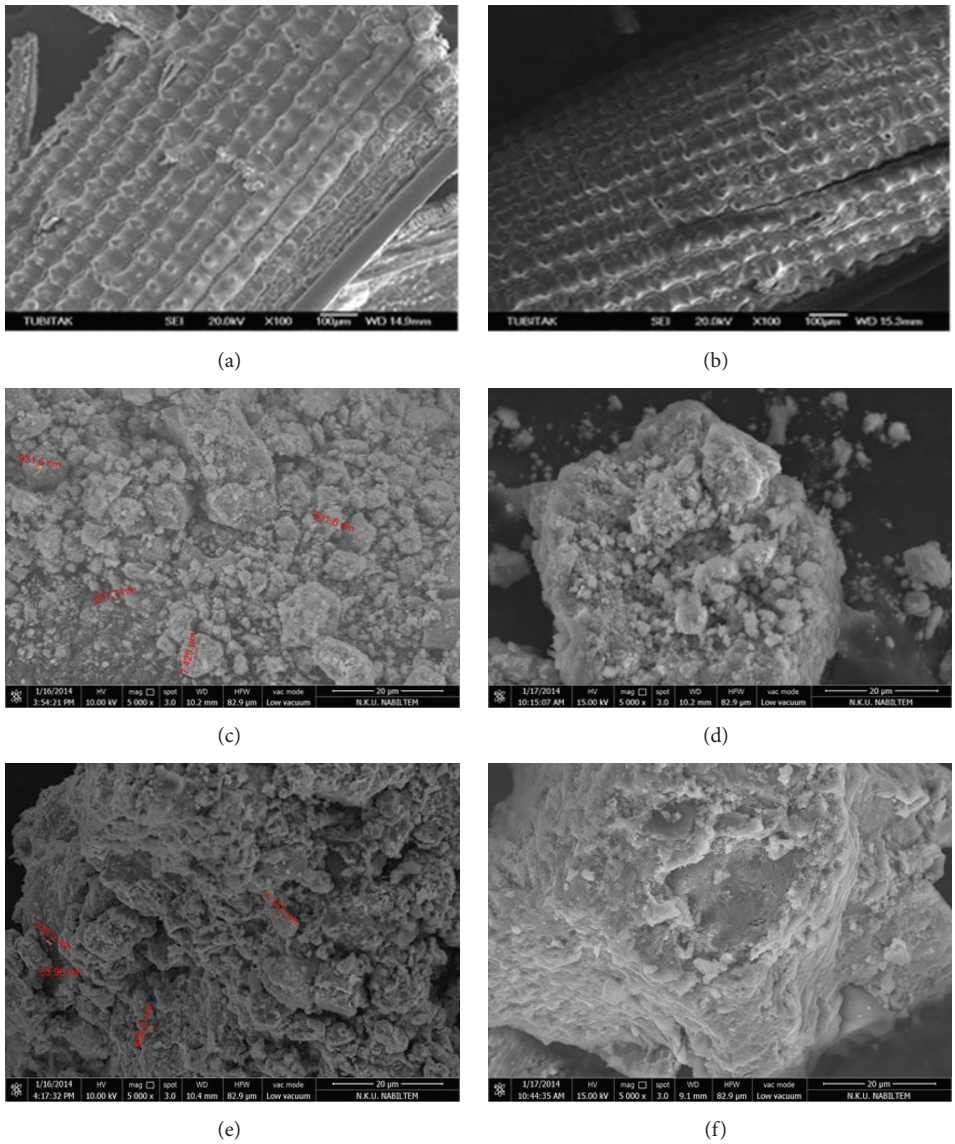

Figure 2: SEM images of the adsorbents: (a) rice husk, (b) rice husk ash burned at 300°C, (c) MNP, (d) MNP after adsorption process (MNP-A), (e) RHA-MNP, and (f) RHA-MNP after adsorption process (RHA-MNP-A).

surface of adsorbents and the anionic dye AR114 [32]. Lower q_e values for AR114 were obtained at basic pH values than acidic pH values. As the pH increased, the MNP and MNP-RHA surface was more negatively charged. So the adsorption of AR114 molecules which is an anionic dye decreases when pH > pH_{pzc} as it is shown in Figure 5. q_e values of MNP and RHA-MNP with an initial dye concentration of 100 mg/L were found to be 91.8 mg/g and 85.5 mg/g, respectively. q_e values for MNP and RHA-MNP for pH 10 were found to be 43.9 mg/g and 43.1 mg/g, respectively. Since the maximum q_e values were obtained at the natural pH (at pH_{pzc} of MNP and RHA-MNP) these pH values were selected for all subsequent AR114 adsorption experiments.

The effect of initial dye concentration for the adsorption of AR114 on MNP and RHA-MNP is shown in Figure 6. q_e (mg/g) values onto MNP and RHA-MNP, by the increase in the dye concentration from 20 mg/L to 100 mg/L, were increased from 13.9 mg/g to 91.8 mg/g and from 17.4 mg/g to 85.5 mg/g, respectively. This is because of the increasing driving force due to the increased dye concentration. An increase in the initial dye concentration increases the interaction between the adsorbent and dye [33]. Initial dye concentration provides a driving force to eliminate the mass transfer of AR114 between the liquid and solid phases.

The effects of contact time according to initial dye concentration for the adsorption of AR114 are shown in Figure 7. As it is seen equilibrium concentration was reached in 30 minutes for MNP and was reached in 90 minutes for RHA-MNP. The adsorption rate increases as the driving force increases due to the increased initial dye concentration. The dye in the solution, with a low initial concentration, interacts with the binding sites and therefore the high adsorption

Table 4: Constants of Langmuir and Freundlich isotherms.

Adsorbent	Langmuir isotherm			Freundlich isotherm		
	q_{max} (mg/g)	K_L (L/g)	R^2	K_f (mg/g)	$1/n$	R^2
MNP	111	0.197	0.9337	20.53	0.53	0.9933
RHA-MNP	111	0.110	0.9930	14.36	0.57	0.9849

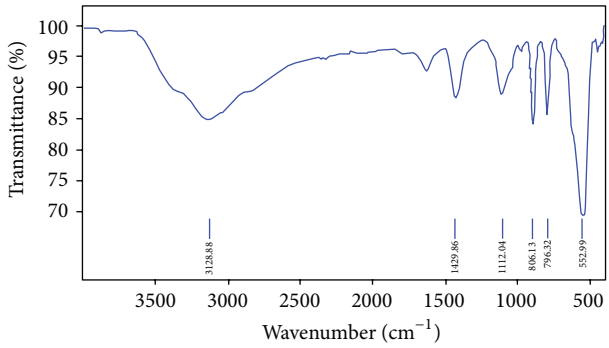

Figure 3: FT-IR spectrum for MNP.

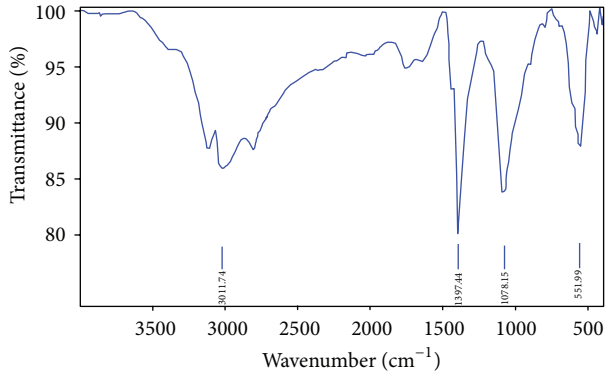

Figure 4: FT-IR spectrum for RHA-MNP.

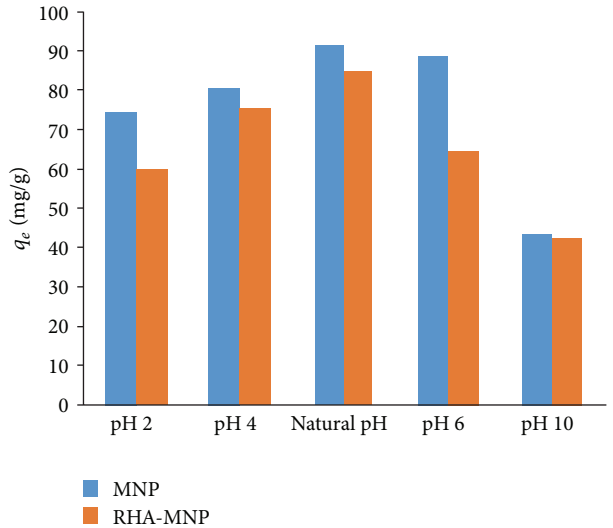

Figure 5: The variation of q_e values depending on pH values of MNP and RHA-MNP.

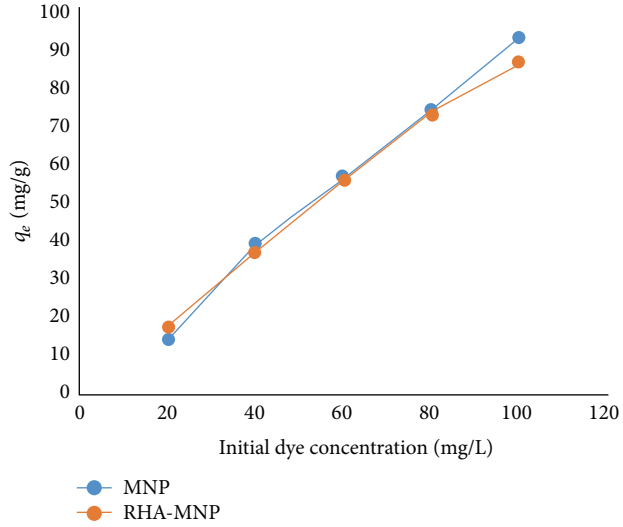

Figure 6: The effect of initial dye concentration for the adsorption of AR114.

rate is obtained [33]. However, in high initial concentrations, binding sites get saturated; therefore, the adsorption rate decreases. It is a result of the formation of the binding sites with low energy due to the increased dye concentration [34].

3.3. Adsorption Isotherms. Langmuir and Freundlich isotherm plots are presented in Figures 8 and 9. The isotherm constants were calculated from the linear form of each model and q_{max} and K_L values for Langmuir isotherm, K_f and $1/n$ values for Freundlich isotherm, and R^2 values for both isotherms are given in Table 4. As can be seen from R^2 values given in Table 4, Freundlich model yielded better fit than the Langmuir model for the adsorption of AR114 on MNP. R^2 values of MNP for Langmuir and Freundlich isotherms are 0.93 and 0.99, respectively. On the other hand R^2 values of RHA-MNP indicate consistency of Langmuir isotherm. Langmuir adsorption capacity was found to be 111 mg dye/g adsorbent for two of the adsorbents. According to results impregnating Fe_3O_4 onto rice husk ash did not change the adsorption capacity.

The characteristics of the Langmuir isotherm could be expressed by a separation factor, R_L, which is defined as [35]

$$R_L = \frac{1}{1 + K_L C_0}, \tag{11}$$

where C_0 is any adsorbate concentration at which the adsorption is carried out. Favorable adsorption is indicated by $0 < R_L < 1$ [36]. The R_L values were found to be between 0.048

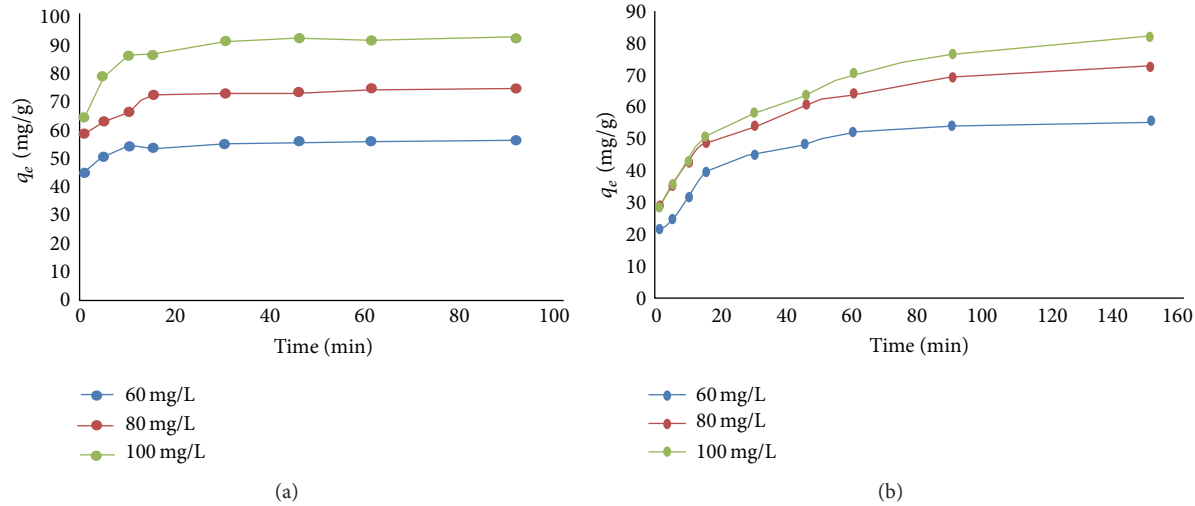

Figure 7: The effect of contact time for the adsorption of AR114 onto MNP (a) and RHA-MNP (b) (at natural pH).

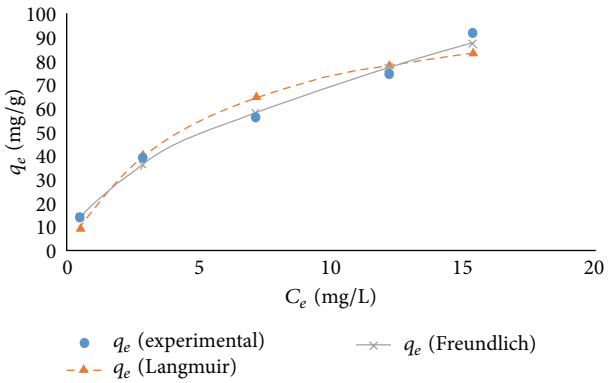

Figure 8: Isotherm plots for the adsorption of AR114 with MNP (natural pH, C_0 = 20, 40, 60, 80, and 100 mg/L, and m = 1 g/L)

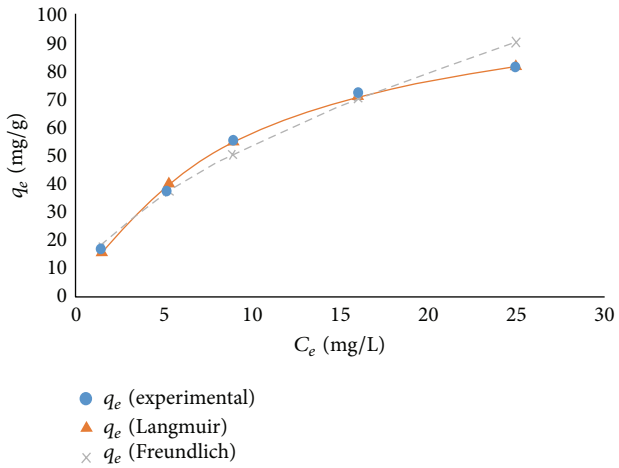

Figure 9: Isotherm plots for the adsorption of AR114 with RHA-MNP (natural pH, C_0 = 20, 40, 60, 80, and 100 mg/L, and m = 1 g/L).

and 0.8 for MNP and between 0.08 and 0.31 for RHA-MNP for initial concentrations of 20, 40, 60, 80, and 100 mg/L (data not shown). R_L values between 0 and 1 show favorable adsorption of AR114 on RHA-MNP and MNP.

K_f and $1/n$ values indicate the adsorption capacity and adsorption density, respectively. $1/n$ values for AR114 adsorption for MNP and RHA-MNP are given as 0.53 and 0.57 in Table 4, respectively. Being smaller than 1, $1/n$ value indicates the convenience of the adsorbents for the dye removal [37]. The consistency of Freundlich isotherm for MNP proves that the surface of the adsorbent consists of small, heterogeneous pores that resemble each other [38].

Table 5 gives the q_{max} value for AR114 adsorption on MNP and RHA-MNP obtained in this study in comparison with the q_{max} values obtained in the other studies carried out with various adsorbents. As can be seen from Table 5, the maximum adsorption capacity (q_{max}) of MNP and RHA-MNP has the value of 111 mg/g for adsorption of AR114. When the adsorption capacity of MNP and RHA-MNP is compared with other adsorbents, it can be understood that these adsorbents possess good adsorption capacity for AR114 dye and rice husk which is a waste could be used as an adsorbent in terms of environmental solutions.

Table 5: Adsorption capacities obtained from present study and other studies for the removal of AR114.

Adsorbent	q_{max} (mg/g)	Reference
Activated pongam seed shells	204.08	[20]
Activated cotton seed shells	153.85	[20]
Activated sesame seed shells	102.04	[20]
Activated carbon-charcoal	101	[21]
Acid activated Eichornia crassipes	112.3	[22]
Filtrasorb F 400	103.5	[23]
MNP	111	This study
RHA-MNP	111	This study

3.4. Adsorption Kinetics. Kinetic studies give valuable information about the mechanism and rate of adsorption

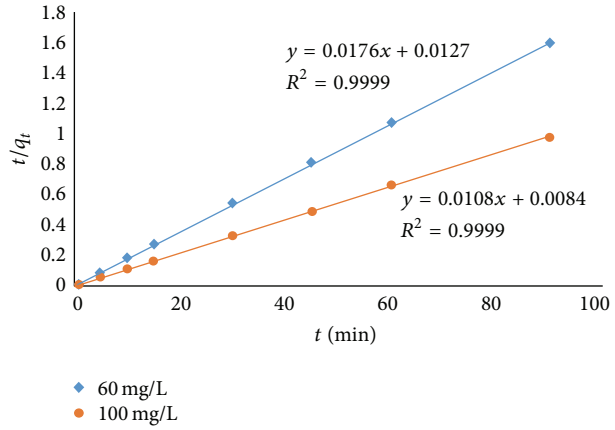

Figure 10: Plot of pseudo-second-order equation for adsorption of AR114 on MNP at different initial dye concentrations (natural pH, C_0 = 60 and 100 mg/L, and m = 1 g/L).

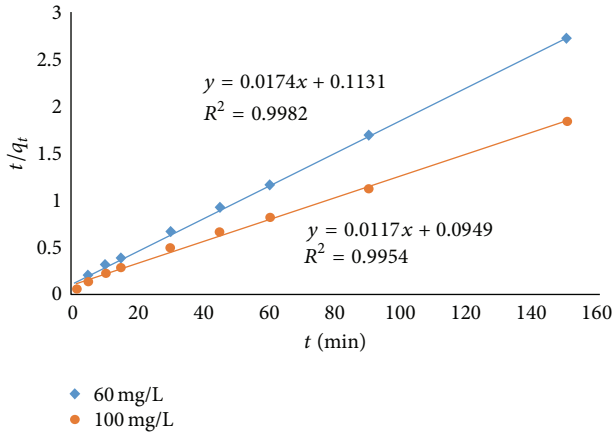

Figure 11: Plot of pseudo-second-order equation for adsorption of AR114 on RHA-MNP at different initial dye concentrations (natural pH, C_0 = 60 and 100 mg/L, and m = 1 g/L).

processes. Adsorption rate (k) and equilibrium adsorption capacity (q_e) which are very important in choosing a better material as a good adsorbent can be calculated by kinetic models [39, 40]. Kinetics of AR114 adsorption on the MNP and RHA-MNP were analyzed using pseudo-first-order and pseudo-second-order kinetics. Results of adsorption kinetic models are given in Figures 10 and 11 and Table 6. Figures 10 and 11 give the linear plots' pseudo-second-order equations for adsorption of AR114 onto MNP and RHA-MNP for the initial concentrations of 60 mg/L and 100 mg/L.

As given in Table 6, R^2 of the pseudo-second-order equations were 0.99 which were close to unity and bigger than pseudo-first-order kinetic model for both adsorbents. For this reason figures related to the pseudo-first-order equations were not shown. As it could be seen from Table 6 the calculated data ($q_{e,cal}$) agreed well with the experimental data ($q_{e,exp}$) for second-order kinetics. As it is shown from Table 6 the adsorption capacities increased with the initial concentration of the AR114 dye. This shows the favorable

Table 6: Kinetic parameters for the adsorption of AR114 on MNP and RHA-MNP (C_0 = 60, 100 mg/L, m = 1 g/L, and natural pH).

MNP				
Pseudo-first-order model				
C_0 (mg/L)	$q_{e,exp}$ (mg/g)	$q_{e,calc}$ (mg/g)	k_1 (min^{-1})	R^2
60	56.06	6.75	0.0513	0.9178
100	91.81	17.48	0.0842	0.6626
Pseudo-second-order model				
C_0 (mg/L)	$q_{e,calc}$ (mg/g)	h (g/mg min)	k_2 (g/mg min)	R^2
60	56.82	78.74	0.024	0.9999
100	92.59	119.05	0.014	0.9999
RHA-MNP				
Pseudo-first-order model				
C_0 (mg/L)	$q_{e,exp}$ (mg/g)	$q_{e,calc}$ (mg/g)	k_1 (min^{-1})	R^2
60	55.39	32.58	0.035	0.9921
100	85.54	53.59	0.026	0.9934
Pseudo-second-order model				
C_0 (mg/L)	$q_{e,calc}$ (mg/g)	h (g/mg min)	k_2 (g/mg min)	R^2
60	57.47	8.842	0.002	0.9982
100	85.47	10.237	0.001	0.9954

adsorption at high concentration [41]. The values of k_2 decrease with the increasing initial concentrations. As stated in literature, at higher concentrations, the competition for the surface active sites was high and at lower concentrations competition for the sorption surface sites was low, and consequently lower k_2 values were obtained [39]. The higher adsorption rate constant k_2 demonstrated faster removal rates of AR114 with lower concentrations [42].

4. Conclusion

The removal of AR114 by adsorption process, using the magnetic nanoparticle (RHA-MNP) which is produced from rice husk ash burned at 300°C as support material and the magnetic nanoparticle (MNP, Fe_3O_4), was studied. The results are summarized below:

(i) MNP contains 62.99% of Fe, while RHA-MNP contains 40.10% of Fe.

(ii) MNP contains nanosized pores. After the adsorption process, an insensible decrease was observed in the porosity of the surface; and heterogeneous, planar formations occurred. Although RHA-MNP structurally resembles MNP, it was estimated that rice husk ash settles on the active pores of MNP. As the dyes are held in the pores of RHA-MNP-A, it has a less porous and homogenous pattern.

(iii) The maximum q_e values for each adsorbent were obtained without correcting pH (natural pH). Natural pH values were equal to pH_{pzc} for two of the adsorbents. The adsorption capacity decreases generally for each adsorbent in high pH values, since negatively charged OH^- ions, which are above pH_{pzc}, and

negatively charged dye ions are competing with each other.

(iv) Both Langmuir and Freundlich isotherms were observed to be convenient to each adsorbent; however Freundlich model yielded better fit for the adsorption of AR114 on MNP and Langmuir model yielded better fit for the adsorption of AR114 on RHA-MNP. Langmuir adsorption capacity was found to be 111 mg dye/g adsorbent for both adsorbents. The consistency of Freundlich isotherm for MNP indicates that the surface of the adsorbent consists of small heterogeneous pores that resemble each other. Similarly, the consistency of Langmuir isotherm for RHA-MNP indicates that surface of adsorbent consists of homogeneous pores.

(v) Kinetic data were adequately fitted by the pseudo-second-order kinetic model. It is found that k_2 values decrease with increasing initial concentration for adsorption of AR114 on MNP and RHA-MNP. It shows that the adsorption process most probably occurs with the surface alteration reaction till the functional areas on the surface are completely filled. Then, the dye molecules are diffused into the adsorbents with various interactions (complex formation, hydrogen bonds, hydrophobic interactions, etc.).

(vi) It can be concluded that RHA-MNP which is a waste could be used as low-cost adsorbent to remove AR114 from aqueous solution.

Competing Interests

The authors declare that they have no competing interests.

Acknowledgments

This research was funded by NKU-BAP Project no. NKUBAP.00.17.AR.12.07.

References

[1] M. M. El-Halwany, "Study of adsorption isotherms and kinetic models for Methylene Blue adsorption on activated carbon developed from Egyptian rice hull (Part II)," *Desalination*, vol. 250, no. 1, pp. 208–213, 2010.

[2] K. Y. Foo and B. H. Hameed, "Utilization of rice husk ash as novel adsorbent: a judicious recycling of the colloidal agricultural waste," *Advances in Colloid and Interface Science*, vol. 152, no. 1-2, pp. 39–47, 2009.

[3] T.-H. Liou and S.-J. Wu, "Characteristics of microporous/mesoporous carbons prepared from rice husk under base- and acid-treated conditions," *Journal of Hazardous Materials*, vol. 171, no. 1–3, pp. 693–703, 2009.

[4] M. Kim, S. H. Yoon, E. Choi, and B. Gil, "Comparison of the adsorbent performance between rice hull ash and rice hull silica gel according to their structural differences," *LWT—Food Science and Technology*, vol. 41, no. 4, pp. 701–706, 2008.

[5] S. T. Ong, C. K. Lee, and Z. Zainal, "Removal of basic and reactive dyes using ethylenediamine modified rice hull," *Bioresource Technology*, vol. 98, no. 15, pp. 2792–2799, 2007.

[6] D. Özdeş, A. Gundogdu, B. Kemer, C. Duran, H. B. Senturk, and M. Soylak, "Removal of Pb(II) ions from aqueous solution by a waste mud from copper mine industry: equilibrium, kinetic and thermodynamic study," *Journal of Hazardous Materials*, vol. 166, no. 2-3, pp. 1480–1487, 2009.

[7] D. Kalderis, D. Koutoulakis, P. Paraskeva et al., "Adsorption of polluting substances on activated carbons prepared from rice husk and sugarcane bagasse," *Chemical Engineering Journal*, vol. 144, no. 1, pp. 42–50, 2008.

[8] G. Kaykioğlu and E. Güneş, "Kinetic and equilibrium study of methylene blue adsorption using $H_2SO_4^-$ activated rice husk ash," *Desalination and Water Treatment*, vol. 57, no. 15, pp. 7085–7097, 2016.

[9] J. Hu, G. Chen, and I. M. C. Lo, "Selective removal of heavy metals from industrial wastewater using maghemite nanoparticle: performance and mechanisms," *Journal of Environmental Engineering*, vol. 132, no. 7, pp. 709–715, 2006.

[10] Y. Feng, J.-L. Gong, G.-M. Zeng et al., "Adsorption of Cd (II) and Zn (II) from aqueous solutions using magnetic hydroxyapatite nanoparticles as adsorbents," *Chemical Engineering Journal*, vol. 162, no. 2, pp. 487–494, 2010.

[11] P. Panneerselvam, N. Morad, and K. A. Tan, "Magnetic nanoparticle (F_3O_4) impregnated onto tea waste for the removal of nickel(II) from aqueous solution," *Journal of Hazardous Materials*, vol. 186, no. 1, pp. 160–168, 2011.

[12] N. M. Mahmoodi, B. Hayati, M. Arami, and H. Bahrami, "Preparation, characterization and dye adsorption properties of biocompatible composite (alginate/titania nanoparticle)," *Desalination*, vol. 275, no. 1–3, pp. 93–101, 2011.

[13] R. Sandoval, A. M. Cooper, K. Aymar, A. Jain, and K. Hristovski, "Removal of arsenic and methylene blue from water by granular activated carbon media impregnated with zirconium dioxide nanoparticles," *Journal of Hazardous Materials*, vol. 193, pp. 296–303, 2011.

[14] M. Uğurlu, M. H. Karaoğlu, and İ. Kula, "UV/H_2O_2/TiO_2/Sep. Nanopartikül Kullanılarak Zeytin Karasuyunda Fotokatalitik Bozunma ve Renk Giderimi," *Ekoloji*, vol. 19, no. 77, pp. 97–106, 2010 (Turkish).

[15] R. Salehi, M. Arami, N. M. Mahmoodi, H. Bahrami, and S. Khorramfar, "Novel biocompatible composite (Chitosan-zinc oxide nanoparticle): preparation, characterization and dye adsorption properties," *Colloids and Surfaces B: Biointerfaces*, vol. 80, no. 1, pp. 86–93, 2010.

[16] X. J. Wang, Y. Wang, X. Wang et al., "Microwave-assisted preparation of bamboo charcoal-based iron-containing adsorbents for Cr(VI) removal," *Chemical Engineering Journal*, vol. 174, no. 1, pp. 326–332, 2011.

[17] G. Absalan, M. Asadi, S. Kamran, L. Sheikhian, and D. M. Goltz, "Removal of reactive red-120 and 4-(2-pyridylazo) resorcinol from aqueous samples by Fe_3O_4 magnetic nanoparticles using ionic liquid as modifier," *Journal of Hazardous Materials*, vol. 192, no. 2, pp. 476–484, 2011.

[18] V. K. Gupta and A. Nayak, "Cadmium removal and recovery from aqueous solutions by novel adsorbents prepared from orange peel and Fe_2O_3 nanoparticles," *Chemical Engineering Journal*, vol. 180, pp. 81–90, 2012.

[19] M. H. Do, N. H. Phan, T. D. Nguyen et al., "Activated carbon/Fe_3O_4 nanoparticle composite: fabrication, methyl orange removal and regeneration by hydrogen peroxide," *Chemosphere*, vol. 85, no. 8, pp. 1269–1276, 2011.

[20] N. Thinakaran, P. Panneerselvam, P. Baskaralingam, D. Elango, and S. Sivanesan, "Equilibrium and kinetic studies on the

removal of Acid Red 114 from aqueous solutions using activated carbons prepared from seed shells," *Journal of Hazardous Materials*, vol. 158, no. 1, pp. 142–150, 2008.

[21] K. K. H. Choy, G. McKay, and J. F. Porter, "Sorption of acid dyes from effluents using activated carbon," *Resources, Conservation and Recycling*, vol. 27, no. 1-2, pp. 57–71, 1999.

[22] N. Rajamohan, M. Rajasimman, R. Rajeshkannan, and B. Sivaprakash, "Kinetic modeling and isotherm studies on a batch removal of acid red 114 by an activated plant biomass," *Journal of Engineering Science and Technology*, vol. 8, no. 6, pp. 778–792, 2013.

[23] K. K. H. Choy, J. F. Porter, and G. McKay, "Langmuir isotherm models applied to the multicomponent sorption of acid dyes from effluent onto activated carbon," *Journal of Chemical & Engineering Data*, vol. 45, no. 4, pp. 575–584, 2000.

[24] I. Langmuir, "The adsorption of gases on plane surfaces of glass, mica and platinum," *The Journal of the American Chemical Society*, vol. 40, no. 9, pp. 1361–1403, 1918.

[25] H. Aydin, Y. Bulut, and Ç. Yerlikaya, "Removal of copper (II) from aqueous solution by adsorption onto low-cost adsorbents," *Journal of Environmental Management*, vol. 87, no. 1, pp. 37–45, 2008.

[26] H. M. F. Freundlich, "Over the adsorption in solution," *The Journal of Physical Chemistry A*, vol. 57, Article ID 385470, 1906.

[27] S. S. Gupta and K. G. Bhattacharyya, "Kinetics of adsorption of metal ions on inorganic materials: a review," *Advances in Colloid and Interface Science*, vol. 162, no. 1-2, pp. 39–58, 2011.

[28] S. Chandrasekhar and P. N. Pramada, "Rice husk ash as an adsorbent for methylene blue-effect of ashing temperature," *Adsorption*, vol. 12, no. 1, pp. 27–43, 2006.

[29] İ. Karaman, *Physical activation of Soma lignite and dye adsorption onto activated product [M.S. thesis]*, Ankara University, Institute of Natural Science, 2010.

[30] S. C. R. Santos, V. J. P. Vilar, and R. A. R. Boaventura, "Waste metal hydroxide sludge as adsorbent for a reactive dye," *Journal of Hazardous Materials*, vol. 153, no. 3, pp. 999–1008, 2008.

[31] T. M. Petrova, L. Fachikov, and J. Hristov, "The magnetite as adsorbent for some hazardous species from aqueous solutions: a review," *International Review of Chemical Engineering (I.RE.CH.E.)*, vol. 3, no. 2, pp. 134–152, 2011.

[32] J. Xu, P. Wu, E. Ye, B. Yuan, and Y. Feng, "Metal oxides in sample pretreatment," *TrAC Trends in Analytical Chemistry*, vol. 80, pp. 41–56, 2016.

[33] V. C. Srivastava, I. D. Mall, and I. M. Mishra, "Competitive adsorption of cadmium(II) and nickel(II) metal ions from aqueous solution onto rice husk ash," *Chemical Engineering and Processing: Process Intensification*, vol. 48, no. 1, pp. 370–379, 2009.

[34] T. K. Naiya, A. K. Bhattacharya, S. Mandal, and S. K. Das, "The sorption of lead(II) ions on rice husk ash," *Journal of Hazardous Materials*, vol. 163, no. 2-3, pp. 1254–1264, 2009.

[35] G. McKay, H. S. Blair, and J. R. Gardner, "The adsorption of dyes onto chitin in fixed bed columns and batch adsorbers," *Journal of Applied Polymer Science*, vol. 29, no. 5, pp. 1499–1514, 1984.

[36] C. Namasivayam and D. Kavitha, "Removal of Congo Red from water by adsorption onto activated carbon prepared from coir pith, an agricultural solid waste," *Dyes and Pigments*, vol. 54, no. 1, pp. 47–58, 2002.

[37] V. S. Mane, I. D. Mall, and V. C. Srivastava, "Kinetic and equilibrium isotherm studies for the adsorptive removal of Brilliant Green dye from aqueous solution by rice husk ash," *Journal of Environmental Management*, vol. 84, no. 4, pp. 390–400, 2007.

[38] C. K. Jain, A. Kumar, and M. Hayssam Izazy, "Color removal from paper mill effluent through adsorption technology," *Environmental Monitoring and Assessment*, vol. 149, no. 1–4, pp. 343–348, 2009.

[39] J. Chang, J. Ma, Q. Ma et al., "Adsorption of methylene blue onto Fe_3O_4/activated montmorillonite nanocomposite," *Applied Clay Science*, vol. 119, pp. 132–140, 2016.

[40] K. A. Tan, N. Morad, T. T. Teng, and I. Norli, "Synthesis of magnetic nanocomposites (AMMC-Fe_3O_4) for cationic dye removal: optimization, kinetic, isotherm, and thermodynamics analysis," *Journal of the Taiwan Institute of Chemical Engineers*, vol. 54, pp. 96–108, 2015.

[41] Z. Jiang and Y. Li, "Facile synthesis of magnetic hybrid Fe_3O_4/MIL-101 via heterogeneous coprecipitation assembly for efficient adsorption of anionic dyes," *Journal of the Taiwan Institute of Chemical Engineers*, vol. 59, pp. 373–379, 2016.

[42] K. Ouyang, C. Zhu, Y. Zhao, L. Wang, S. Xie, and Q. Wang, "Adsorption mechanism of magnetically separable Fe_3O_4/graphene oxide hybrids," *Applied Surface Science*, vol. 355, pp. 562–569, 2015.